# Inference Offloading for Cost-Sensitive Binary Classification at the Edge

**Vishnu Narayanan Moothedath[1], Umang Agarwal[2], Umeshraja N[2], James Richard Gross[1], Jaya Prakash Champati[3], Sharayu Moharir[2]**

[1]Information Science and Engineering, KTH Royal Institute of Technology, Stockholm, Sweden
[2]Electrical Engineering, Indian Institute of Technology Bombay, Mumbai, India
[3]Computer Science, University of Victoria, Victoria, Canada.

## Abstract

We focus on a binary classification problem in an edge intelligence system where false negatives are more costly than false positives. The system has a compact, locally deployed model, which is supplemented by a larger, remote model, which is accessible via the network by incurring an offloading cost. For each sample, our system first uses the locally deployed model for inference. Based on the output of the local model, the sample may be offloaded to the remote model. This work aims to understand the fundamental trade-off between classification accuracy and these offloading costs within such a hierarchical inference (HI) system. To optimize this system, we propose an online learning framework that continuously adapts a pair of thresholds on the local model's confidence scores. These thresholds determine the prediction of the local model and whether a sample is classified locally or offloaded to the remote model. We present a closed-form solution for the setting where the local model is calibrated. For the more general case of uncalibrated models, we introduce H2T2, an online two-threshold hierarchical inference policy, and prove it achieves sublinear regret. H2T2 is model-agnostic, requires no training, and learns in the inference phase using limited feedback. Simulations on real-world datasets show that H2T2 consistently outperforms naive and single-threshold HI policies, sometimes even surpassing offline optima. The policy also demonstrates robustness to distribution shifts and adapts effectively to mismatched classifiers.

## 1 Introduction

Edge intelligence systems often operate in critical and resource-constrained environments, where inference tasks must carefully balance cost and accuracy. Examples include event detection, typically framed as binary classification with applications such as medical diagnostics, surveillance, and smart cameras detecting theft, where high reliability must be achieved with low cost. For instance, consider a medical scenario where a lightweight local inference model performs radiology screening of patient scans but may struggle with ambiguous or complex cases. Offloading such samples to a more accurate remote model–or a human specialist–can considerably improve reliability, but by incurring significant networking and access costs. The consequences of false positives (FP) and false negatives (FN) are typically asymmetric in such settings. For example, missing an incoming threat or a cancer case may be far costlier than a false alarm. Moreover, retraining or updating the local model to adapt to distribution shifts or cost changes may be impractical due to network limitations or model complexity. As a result, training-independent, inference-time decisions become essential. In some systems, pre-training may not be possible at all, requiring models to learn on the fly (Sturzinger and Satyanarayanan 2024).

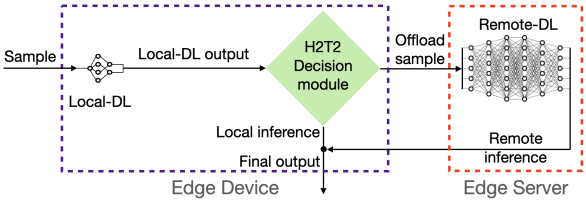


Figure 1: Architecture of the proposed HI Hedge with Two Thresholds (H2T2) offload decision-making policy.

We consider an edge intelligence system with an edge device and a remote server. The device is equipped with a pre-trained local DL (LDL) model tasked with cost-sensitive binary classification. For each sample, it can either make a local decision using the LDL output or offload it–at a cost–to a larger, more accurate remote DL (RDL) model. We aim to design an inference-time offloading policy with asymmetric FP and FN costs that selectively offload ambiguous samples based on the LDL output. We use Hierarchical Inference (HI) (Moothedath, Champati, and Gross 2024; Beytur et al. 2024; Al-Atat et al. 2024), a post-hoc meta learning framework where each sample is first sent to the LDL, and the decision to offload to the RDL is made based on the LDL's output; see Figure 1. Prior HI works learned a threshold and offloads a sample if the LDL's confidence (e.g., maximum softmax value) of its decision falls below it.

### Related Works

HI has received considerable attention (Nikoloska and Zlatanov 2021; Letsiou et al. 2024; Al-Atat et al. 2023; Moothedath, Champati, and Gross 2024; Beytur et al. 2024; Al-Atat et al. 2024; Behera et al. 2025; Datta, Moharir, and Champati 2025), particularly within the edge computing community. Nikoloska and Zlatanov; Al-Atat et al.; Behera et al. assumed a fixed offloading cost per sample and

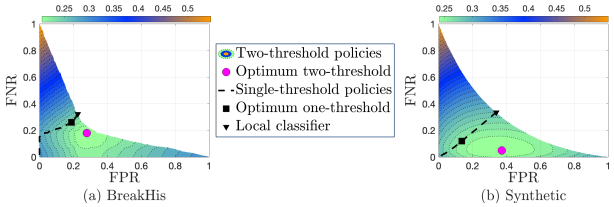


Figure 2: FPR vs. FNR and average cost of single- and two-threshold policies on (a) BreakHis, and (b) synthetic configurations from TABLE 2. Normalized costs of false positive, false negative, and offload are 0.7, 1, and 0.3, respectively.

used a predetermined threshold–computed from the training data–on the maximum softmax value of the LDL to make the offloading decision. To handle the varying offloading costs and distribution drifts between training and inference phases, Moothedath, Champati, and Gross; Beytur et al.; Al-Atat et al.; Letsiou et al. investigated learning the optimum threshold online. Moothedath, Champati, and Gross formulated HI as a variant of the classical Prediction with Expert Advice (PEA) (Cesa-Bianchi and Lugosi 2006) and provided dataset-dependent regret bounds. Al-Atat et al. provided improved regret bounds for the problem, considering a more general setting with random and potentially correlated offloading costs. Beytur et al. extended HI to multiple devices and studied maximizing accuracy subject to an average offloading cost constraint. In contrast to existing work on HI, we consider asymmetric costs for FPs and FNs.

Our work is also related to the Learning to Reject (L2R) and Learning to Defer (L2D) problems Cortes, DeSalvo, and Mohri; Saerens, Latinne, and Decaestecker; Ramaswamy, Tewari, and Agarwal; Ni et al.; Narasimhan et al., which focus on training models with an option to reject, or defer to an expert model–at some cost. In contrast, ours is a meta-learning framework proposed for the inference phase, where the pre-trained LDL is unaltered, and it does not require offline RDL inferences. This allows for the use of off-the-shelf models on the edge device and the server. In contrast to cost-sensitive classification (Elkan 2001), our problem requires ambiguity-awareness not only for cost-sensitive classification but also to make the offloading decision. Finally, our framework handles Out-of-Distribution (OOD) samples at inference time, allows independent costs for local processing, offloading, false positives, and false negatives, and allows the offloading cost to be random and unknown a priori. We summarize the difference with related works in Table 1.

While prior HI works use the LDL output to make naive *argmax*-based LDL inference when not offloading, we use it to make our own cost-sensitive decisions–serving as both an offloading and a local inference policy. More importantly, all HI works use a single threshold for offloading decisions. We argue that, for cost-sensitive classification, using a single threshold results in sub-optimal solutions. To illustrate this, in Fig. 2 we use two dataset-classifier combinations and show the false-positive rates (FPRs), false negative rates (FNRs), and the average costs achievable by single-threshold and two-threshold policies. While single-threshold

| Related work category | AA | AC | IT | DMA |
|---|---|---|---|---|
| Rejection(L2R), Deferral(L2D) | ✓ | × | × | × |
| Cost-Sensitive Classification | × | ✓ | × | × |
| HI–Single Threshold | ✓ | × | ✓ | ✓ |
| H2T2 (proposed) | ✓ | ✓ | ✓ | ✓ |

Table 1: Comparison of the proposed policy with related work categories across key properties: ambiguity-aware (AA), asymmetric costs (AC), inference-time learning (ITL), and dataset & model agnostic (DMA).

policies can reduce FPR and FNR, even the best single-threshold policy cannot achieve the lowest possible overall cost. Instead, we propose a two-threshold HI decision rule and present a sub-linear regret algorithm to solve the problem at hand.

### Our Contributions

Our key contributions are outlined as follows:

- For calibrated LDL models, we derive a two-threshold rule for the softmax value that minimizes the Bayesian expected cost. When FP and FN costs are equal and offloading cost is constant, this rule reduces to Chow's rule for classification with rejection (Chow 2003).
- Motivated by this, we propose a two-threshold-based HI policy called H2T2 to solve the problem and show that it has $O(T^{\frac{2}{3}})$ regret. Since ground truth labels are unavailable during inference, H2T2 estimates local misclassifications by offloading a fraction of input samples.
- Experiments on real-world and synthetic datasets demonstrate lower costs of H2T2 compared to the baseline policies, and in some cases, even offline single-threshold optima. While some cost regions favor naive policies, these regions are unknown a priori. We also show that H2T2 cost gains are significant for out-of-distribution data.

In the following sections, we present the problem setup, theoretical results for calibrated models, the proposed algorithm with regret analysis, and experimental evaluation. Proofs are in the appendix; additional results and details are in the supplementary material.

## 2 Problem Setting

We consider a system consisting of an edge device and an edge server. The device needs to infer relevant information from each sample arriving periodically, which is then used to make control decisions. This work focuses on the case where this inference task is a cost-sensitive binary classification or event detection. The system is equipped with two DL models trained for this task: a local DL (LDL) deployed on the device, and a remote DL (RDL) deployed on the server. Given the memory and computing constraints of the device, the LDL is lightweight and, therefore, has lower accuracy than the RDL. We focus on the HI framework, where each sample is first processed by the LD. Based on its output, the system either makes a local inference or offloads the sample to the RDL for better inference.

**Inference Task** Assume samples $x_t$ arrive i.i.d. in time slots indexed by $t$. The goal of the classifier is to map each sample to one of two possible classes, 0 and 1. To this end, the model outputs a softmax tuple $(f_0(x_t), f_1(x_t)) \in \mathbb{R}^2$ with $0 \leq f_0(x_t), f_1(x_t) \leq 1$, and $f_0(x_t) + f_1(x_t) = 1$. In the remainder of this work, we define the class 1 as the class or event of interest and $f_t \coloneqq f_1(x_t)$ as the corresponding LDL output. We assume that the model outputs are expressed using $b$ bits and therefore are quantized into $2^b$ values. This is true for any practical system and has also been assumed in related literature.

**Loss Function** We denote the LDL and RDL models by the binary classifiers $h_l(.)$ and $h_r(.)$. For each sample $x_t$, we either use $h_l(x_t)$ or offload the sample and use $h_r(x_t)$ as our inference. In the absence of knowledge of the ground truth class for each sample, we treat the inference of the RDL as a proxy for this ground truth. This is justified by the fact that in any non-trivial scenario, the LDL aims to achieve the performance of the RDL, and no more. Under this consideration, we have two types of classification errors that can occur when the inference is made locally:

- False-positive (FP), when, $h_l(x_t) = 1$ and $h_r(x_t) = 0$,
- False-negative (FN), when, $h_l(x_t) = 0$ and $h_r(x_t) = 1$.

We use $\delta_1, \delta_{-1}$ and $\beta_t$ to denote the normalized false positive, false negative, and offload cost at time $t$. Here, $\beta_t < \beta$ is generated by an oblivious adversary. Normalization is done by subtracting the common LDL processing cost and scaling by the maximum cost, mapping all values to $[0, 1]$. When a local inference is made, the system incurs a loss of $\phi_t$:

$$\phi_t = \begin{cases} \delta_1 & \text{if FP} \\ \delta_{-1} & \text{if FN} \\ 0 & \text{otherwise.} \end{cases} \tag{1}$$

We assume that $\beta_t$ is presented to the policy at the start of round $t$. The system is trivial when $\beta_t \geq \max\{\delta_1, \delta_{-1}\}$, enabling an assumption of $\beta_t \leq \beta = 1$. Let $\pi$ denote the policy (or algorithm) making offloading decisions and $l_t(\pi)$ denote the incurred cost at round $t$. It follows that

$$l_t(\pi) = \begin{cases} \phi_t & \text{if } h_l(x_t) \text{ is used} \\ \beta_t & \text{otherwise.} \end{cases} \tag{2}$$

The corresponding cumulative loss $L_T(\pi) = \sum_{t=1}^{T} l_t(\pi)$. In the remainder of this work, we omit $\pi$ and refer to these as $l_t$ and $L_T$, for simplicity.

### Threshold-based Policies and Performance Metric

Recall that for each sample, LDL outputs a score $f_t$ corresponding to class 1. It follows that if $f_t$ is large (close to 1) or small (close to 0), it is very likely that the ground truth is 1 or 0. On the other hand, intermediate values of $f_t$ imply ambiguity. Motivated by this, we focus on threshold-based HI policies where the offloading decision in each slot $t$ is governed by a tuple $\vec{\theta} \coloneqq (\theta_l, \theta_u)$, where $0 \leq \theta_l \leq \theta_u \leq 1$. A sample is offloaded if $\theta_l \leq f_t < \theta_u$, predicted as class 1 if $f_t \geq \theta_u$, and class 0 otherwise. Our goal in this work is to learn these thresholds online.

We say that a policy is a fixed-threshold (fixed-$\vec{\theta}$) policy if $\vec{\theta}$ does not change over the time-horizon of interest. For simplicity, we overload the notation $l_t$ from (2) and reuse it to denote $l_t(\vec{\theta})$ and $L_t(\vec{\theta})$, the instantaneous and cumulative losses incurred, respectively, by a fixed-threshold policy that uses $\vec{\theta}$ as the threshold tuple. It follows that

$$l_t(\vec{\theta}) = \begin{cases} \beta_t & \text{if } \theta_l \leq f_t < \theta_u, \\ \phi_t & \text{otherwise.} \end{cases} \tag{3}$$

Define $\vec{\theta}^* = (\theta_l^*, \theta_u^*)$ as the thresholds with the lowest expected cumulative loss in the class of fixed-$\vec{\theta}$ policies.

$$\vec{\theta}^* = \arg\min_{\vec{\theta}} \mathbb{E}\left[L_T(\vec{\theta})\right] = \arg\min_{\vec{\theta}} \mathbb{E}\left[\sum_{t=1}^{T} l_t(\vec{\theta})\right]. \tag{4}$$

Unless otherwise mentioned, $\mathbb{E}[.]$ denotes expectation taken over the randomness in the arrival sequence and that in the candidate policy. We use a fixed threshold policy with threshold as $\vec{\theta}^*$ as the baseline to compare the performance of candidate policies. Our performance metric for a candidate policy is regret, denoted by $R_T$, where

$$R_T = \mathbb{E}[L_T] - \mathbb{E}[L_T(\vec{\theta}^*)]. \tag{5}$$

## 3 Optimal Policy Under a Calibrated Model

In this section, we focus on the setting where the LDL is calibrated, i.e., for each sample, the LDL output (softmax value) for each class is equal to the a posteriori probabilities of that sample belonging to that class. Let $\mathcal{X}$ and $\mathcal{Y}$ denote the input space and the label space, respectively. Assume that $(x_t, h_r(x_t))$ is drawn i.i.d from $\mathcal{X} \times \mathcal{Y}$

**Definition 1** (Calibrated Model)**.** *The DL model that generates the softmax values $(1 - f_t, f_t)$ for the sample $x_t$ is calibrated, if $\mathbb{P}(h_r(x_t) = 1 | x_t) = f_t$, $\forall t$.*

We now characterize the optimal HI offloading policy for cost-sensitive classification for calibrated LDL.

**Theorem 1.** *Let $x_t$ denote the sample input to a calibrated LDL. Then, the optimal predictor $h_l^*(x_t)$ is given by*

$$h_l^*(x_t) = \begin{cases} 1, & \text{if } f_t \geq \frac{\delta_1}{\delta_1 + \delta_{-1}}, \\ 0, & \text{otherwise.} \end{cases} \tag{6}$$

*Further, the optimum offloading decision for this setup is to offload the sample when*

$$\theta_l^{*(t)} \coloneqq \frac{\beta_t}{\delta_{-1}} \leq f_t < 1 - \frac{\beta_t}{\delta_1} \coloneqq \theta_u^{*(t)}, \tag{7}$$

*with an associated expected cost of*

$$\mathbb{E}[l_t] = \min\{\beta_t, \delta_1(1 - f_t), \delta_{-1} f_t\}. \tag{8}$$

**Remark 1.** *Theorem 1 implies the following: (i) Offloading does not occur if $\beta_t \geq \frac{\delta_1 \delta_{-1}}{\delta_1 + \delta_{-1}}$, half the harmonic mean of $\delta_1$ and $\delta_{-1}$; (ii) when $\delta_1 = \delta_{-1}$, the decision is equivalent to Chow's rule for classification with rejection, with no offloading if $\beta_t \geq 0.5$, and offloading if and only if $\min\{f_1(x_t), f_0(x_t)\} < \beta_t$. If not offloaded, the prediction is the class with the higher softmax value.*

The key question is its extension to non-calibrated models, where the thresholds must be learned.

Algorithm 1: H2T2: The two threshold HI policy.

$\epsilon$, $\eta$, $\Theta$. ▷ Input
$w_1(\vec{\theta}) = 1 \; \forall \; \vec{\theta} \in \Theta$, and $W_1 = |\Theta|$. ▷ Initialization
**for** $t \geq 1$ **do**
  Observe $f_t$. ▷ LDL inference
  $p_t = \sum_{\theta_l < f_t} \sum_{\theta_u < f_t} w_t(\vec{\theta})$. ▷ Region 3
  $q_t = \sum_{\theta_l \leq f_t} \sum_{\theta_u > f_t} w_t(\vec{\theta})$. ▷ Region 2
  $\psi_t \sim \text{Uniform}(0, 1)$.
  $\zeta_t \sim \text{Bernoulli}(\epsilon)$.
  **if** $\psi_t \leq q_t$ or $\zeta_t = 1$ **then** ▷ Region 2, or exploration
    Offload $x_t$, receive $h_r(x_t)$, and observe $\phi_t$.
    **for all** $\vec{\theta} \in \Theta$ **do**
      Compute $\tilde{l}_t(\vec{\theta})$ using (10). ▷ Pseudo-loss
      $w_{t+1}(\vec{\theta}) = e^{-\eta \tilde{l}_t(\vec{\theta})} w_t(\vec{\theta})$. ▷ Weight updation
    **end for**
    $W_{t+1} = \sum_{\vec{\theta} \in \Theta} w_{t+1}(\vec{\theta})$.
  **else** ▷ Local inference
    **if** $\psi_t \leq q_t + p_t$ **then**
      $h_l(x_t) = 1$. ▷ Region 3
    **else**
      $h_l(x_t) = 0$. ▷ Region 1
    **end if**
  **end if**
**end for**

## 4 The H2T2 Policy

This section relaxes the assumption of a calibrated LDL, proposing instead an online policy that learns the values of the two thresholds. Any policy within our framework must make two decisions: first, whether to offload a given sample; and second, if the sample is not offloaded, the policy has to predict a class based on the LDL's output.

**Algorithm** We present the proposed HI-Hedge with Two Thresholds (H2T2) policy in Algorithm 1. We note that H2T2 maps to the Prediction with Expert Advice (PEA) problem, where the *experts* are the threshold tuples $\vec{\theta}$. We denote the set of experts as $\Theta$. Given $\theta_l \leq \theta_u$, it follows that $|\Theta| = 2^{b-1}(2^b + 1)$ experts. Fig. 3 illustrates three regions of the experts with respect to an observed $f_t$. We maintain weights for all experts. The probability of choosing an expert in a round is proportional to its weight in that round. This process will be discussed shortly.

Under H2T2, given the output of the LDL and the expert (i.e., threshold tuple) chosen in round $t$, denoted with superscript $^{(t)}$, the local prediction $h_l(x_t)$ is defined as follows:

$$h_l(x_t) = \begin{cases} 0, & \text{if } f_t < \theta_l^{(t)} \leq \theta_u^{(t)}, \\ \text{Ambiguous}, & \text{if } \theta_l^{(t)} \leq f_t < \theta_u^{(t)}, \\ 1, & \text{if } \theta_l^{(t)} \leq \theta_u^{(t)} \leq f_t. \end{cases} \tag{9}$$

H2T2 offloads all samples for which $h_l(x_t)$ is ambiguous. Otherwise, it still offloads with a probability $\epsilon$ based on a Bernoulli random variable $\zeta_t \sim \text{Ber}(\epsilon)$. The motivation of this *exploration* step will be explained shortly. If H2T2 does not offload, $h_l(x_t)$ is the predicted class.

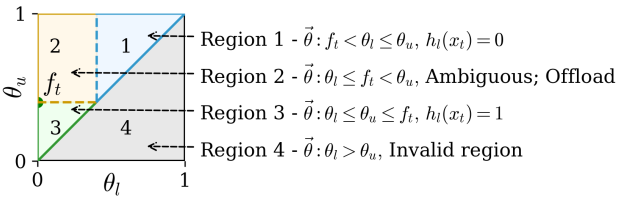


Figure 3: Illustration showing the invalid and three valid regions of experts from (9) with respect to an observed $f_t$.

We now discuss the process of computing the weights under H2T2. Recall that, in our setting, we use the inference of the RDL as a proxy for the ground truth. One of the key challenges in our setting is that this inference is observed only when we offload a sample, and therefore, unlike the classical PEA setting, we learn the loss incurred by the experts only when we offload a sample.

To address this challenge, H2T2 employs two steps: First is the exploration step discussed earlier, where unambiguous samples are randomly offloaded with a probability $\epsilon$. Next, H2T2 maintains an estimated loss $\tilde{l}_t(\vec{\theta})$ for each expert that is updated only with a feedback reception. Let $E_t$ and $O_t$ be indicator random variables denoting exploration and offloading. That is $E_t = 1$ if $\zeta_t = 1$ *and* $f_t \notin [\theta_l^{(t)}, \theta_u^{(t)})$; and $O_t = 1$ if $E_t = 1$ *or* $f_t \in [\theta_l^{(t)}, \theta_u^{(t)})$. Further, Let $\mathbb{1}_{x_t}(\vec{\theta})$ be an indicator random variable that is one if $h_l(x_t)$ would have been ambiguous if the expert chosen in time $t$ was $\vec{\theta}$, i.e., $\theta_l \leq f_t < \theta_u$. Thus, we define

$$\tilde{l}_t(\vec{\theta}) = \begin{cases} \beta_t & \text{if } O_t = 1, \mathbb{1}_{x_t}(\vec{\theta}) = 1, \\ \frac{\phi_t}{\epsilon} & \text{if } E_t = 1, \mathbb{1}_{x_t}(\vec{\theta}) = 0 \\ 0 & \text{otherwise.} \end{cases} \tag{10}$$

Each expert's weight in a round is an exponential function of the cumulative estimated loss of that expert up to that round, with a learning rate $eta$. In our setting, all experts that yield the same $h_l(x_t)$ create contiguous and convex regions, as illustrated in Fig. 3. This simplifies the decision-making process: it suffices to compute the total probability of all experts in each of the three regions to decide whether to offload and to determine the inference of the LDL. For simplicity, we omit the superscript $^{(t)}$ in the notation from here onward.

**Regret analysis** We now provide regret guarantees for H2T2. We first prove the following two lemmas. In Lemma 1, we show that $\tilde{l}_t(\vec{\theta})$ is an unbiased estimator of the loss.

**Lemma 1.** *For all values of $f_t$ and for all $\vec{\theta} \in \Theta$:*

$$\mathbb{E}_\zeta[\tilde{l}_t(\vec{\theta})] = l_t(\vec{\theta}).$$

Let $\tilde{L}_T = \sum_{t=1}^{T} \tilde{l}_t$ be the cumulative estimated loss. Next, we upper bound the difference in the expected values of the cumulative loss and the cumulative estimated loss in Lemma 2. Here, the expectation is over the randomness of both the expert selection and $\zeta$.

**Lemma 2.** *For any policy and time horizon $T$:*

$$\mathbb{E}\left[L_T\right] - \mathbb{E}\left[\tilde{L}_T\right] \leq \epsilon\beta \leq \epsilon T.$$

We use these lemmas to upper bound the regret of H2T2.

**Theorem 2.** *The regret $R_T$ of H2T2 satisfies*

$$R_T \leq \left(\epsilon\beta + \tfrac{\eta}{2\epsilon}\right) T + \tfrac{\ln(|\Theta|)}{\eta}. \tag{11}$$

The regret-minimizing values of $\eta$ and $\epsilon$ can be obtained by setting the partial derivatives of $R_T$ to zero.

**Corollary 1.** *$R_T$ is minimized by $\epsilon^* = \left(\ln(|\Theta|)/2\beta^2 T\right)^{1/3}$ and $\eta^* = \sqrt{2\epsilon^* \ln|\Theta|/T}$. H2T2 with $\eta^*$ and $\epsilon^*$ has $O\left(T^{2/3}\right)$ regret.*

We thus note that H2T2 has sub-linear regret.

## 5 Experimental Results

We evaluate the performance of H2T2 via experiments on the following dataset-model pairs, which we simply refer to by the dataset name.

(a) The Breast Cancer Histopathological Image Classification **(BreakHis)** (Spanhol et al. 2015) contains 7909 images of benign (class 1) and malignant cells. The LDL model is a lightweight MobileNet-based classifier with additional dense and dropout layers.

(b) **Chest** (Mohamed 2025) contains 844 chest CT scan images re-categorized into healthy and cancerous (class 1) classes for our use. The LDL is based on MobileNet, with a size of 13.3 MB including trainable parameters.

(c) **Phishing** (Tiwari 2025; Tan 2018) includes data collected from 5000 phishing and as many legitimate websites, with additional samples for testing. A logistic regression model (56 bytes) is used as LDL.

(d) For the **Synthetic** dataset, we generate softmax-like values using Gaussian mixtures truncated to $(0, 1)$.

(e) **BreaCh** is created by classifying all 7909 BreakHis samples using the model trained on Chest CT scan. It mimics an OOD data scenario with a domain shift for the model trained on Chest CT scan. As a result, unbeknownst to the user, the accuracy drops below 50%, resulting in the misdiagnosis of 38% cancerous tumors.

These are summarised in Table 2. For benchmarking, we implement the following policies:

1. *No Offload*, where the LDL inference is accepted as is;
2. *Full Offload*, where all samples are offloaded;
3. *HI-single threshold*, the state-of-the-art continuum expert HI policy (Moothedath, Champati, and Gross 2024);
4. $\theta^\dagger$, offline optimal single-threshold policy;
5. $\vec{\theta}^*$, offline optimal two-threshold policy;
6. *H2T2*, our proposed policy.

We set $\delta_1 = 0.7$ and $\delta_{-1} = 1$ and use a fixed offloading cost $\beta$ for comparison study. Similar trends are observed for varying $\delta_1$ and $\delta_{-1}$. The quantized threshold resolution is set to $0.0625$, resulting in $|\Theta| < 256$. An increase in resolution did not result in a considerable reduction in average cost for the datasets studied. Since the bound optimizing parameters from 1 do not necessarily minimize regret, we use $\eta^*$ from Corollary 1 and set learning rate $\eta = 1$ without further parameter tuning. For fair comparison, $T = 10^4$ samples from each dataset via uniform sampling. Standard deviation for HI-single threshold and H2T2 are included in all figures, but are negligible. We refer the reader to the supplementary material for further details and additional illustrations.

### Performance Comparison

In Fig. 4, we present the average cost incurred by different policies by varying the fixed offloading cost $\beta \in (0, 0.6)$. We observe that H2T2 outperforms the state-of-the-art HI single-threshold policy and provides a percentage reduction of up to 41% (for Fig. 4(d) at $\beta = 0.6$). However, for Phishing in Fig. 4(c), the improvement is marginal. This is attributed to the policies yielding near-trivial results, as indicated by the overlap of their respective offline optima and the No-offload policy. Interestingly, in two datasets, H2T2 outperforms $\theta^\dagger$, the offline optimal single-threshold policy.

For some $\beta$ values (e.g., $\beta > 0.3$ in BreakHis), the No-offload and Full-offload policies outperform online learning policies. However, these regions are dataset-and model-dependent and unknown a priori.

Note the significant cost reduction achieved by H2T2 for BreaCh in Fig. 4(e) for the OOD data. Being model-agnostic and robust to distribution shifts, H2T2 limits the additional cost of data (or model) mismatch to about $0.12$ (or $0.02$) at $\beta = 0.6$; see Fig. 4(a) and (b). Even when offload is relatively costly ($\beta = 0.6$), we observed that H2T2 reduces FN rate from 38% to around 10%.

## 6 Discussion: Multiclass Classification

We have thus far focused on cost-sensitive binary classification. We now briefly examine extending our setting to multiclass classification with asymmetric pairwise misclassification costs. The overarching objective remains the same: to partition the softmax value space into distinct regions for each class and an additional region for offload.

Let $K$ be the number of classes and $C \in [0, 1]^{K \times K}$ be the normalized cost matrix where $C_{ij}$ is the cost of misclassifying class $i$ as class $j$, and $C_{ii} = 0$, $\forall i$. Let $f$ be the $K \times 1$ softmax vector and $C_k$ denote the $k^{\text{th}}$ column of $C$, representing the cost vector when class $k$ is the prediction. The loss function $l_t$ follows (2), with a modified $\phi_t$ defined as:

$$\phi_t = C_{ij}, \quad \text{if class } i \text{ is predicted as } j. \tag{12}$$

| Dataset | Size | LDL | Accuracy | FP | FN |
|---|---|---|---|---|---|
| BreakHis | 3365 | MobileNet-based | 72% | 10% | 18% |
| Chest | 278 | MobileNet-based | 64% | 16% | 20% |
| Phishing | 1106 | Logistic regression | 75% | 12% | 13% |
| Synthetic | $10^5$ | Naive | 66% | 15% | 19% |
| BreaCh | 7909 | Chest classifier | 45% | 17% | 38% |

Table 2: Different dataset-model pairs used in Fig. 4. Note that BreaCh is intentionally made erroneous.

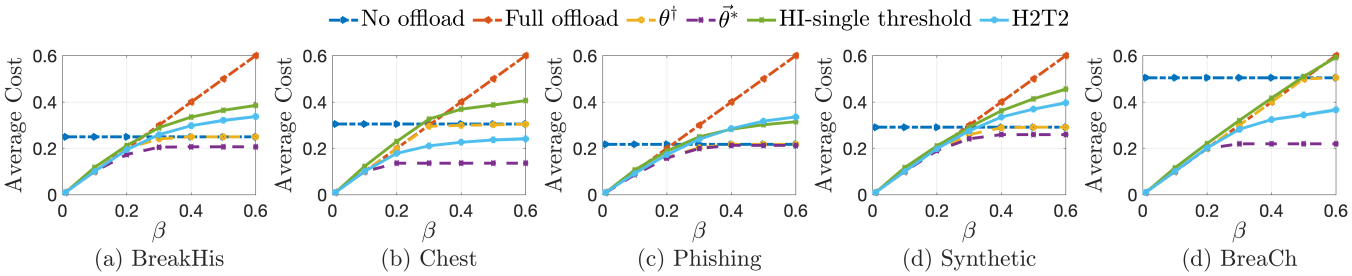


Figure 4: Average cost of H2T2 policy vs. fixed offloading cost $\beta$ for different datasets. Figures (a)-(d) are for in-distribution data, and (e) is for OOD data.

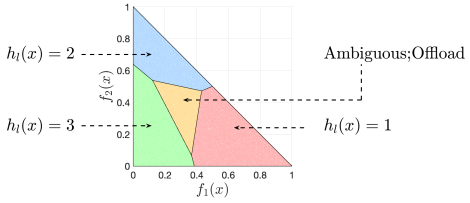


Figure 5: Illustration showing the four regions for a three-class classification by a calibrated LDL, plotted in a plane defined by the (first) two independent softmax components. Linear boundaries bound the regions, and the inferences are marked within. $\delta_1 = 0.7, \delta_{-1} = 1, \beta = 0.4$. A suitable cost matrix $C$ is selected from a random sample for clarity.

**Theorem 3.** *The optimal predictor $h_l^*(x_t)$ of a calibrated LDL designed for a $K$-class classification task is given by:*

$$h_l^*(x_t) = \arg\min_k f^T C_k. \tag{13}$$

*Further, the optimum offloading decision for this setup is to offload the sample when $\min_k f^T C_k > \beta_t$ with an associated expected cost of $\mathbb{E}[l_t] = \min\{\beta_t, \min_k f^T C_k\}$.*

For calibrated models, this yields $K+1$ decision regions bounded by $(K-2)$-dimensional simplexes in closed-form. For instance, in the binary case ($K = 2$) of previous sections, we saw three regions bounded by 2 points; for $K=3$, there are four regions bounded by line segments as illustrated in Fig. 5. Note that we could represent these regions in $K$-dimensions on the $K-1$-dimensional standard (probability) simplex $f^T\vec{1} = 1$, or remove an independent variable and represent it directly in $K-1$ dimensions.

In the case of uncalibrated models, the boundaries of these regions are not known a priori. Similar to the binary setting, we consider a class of experts for each of these boundaries, and design a similar PEA policy to learn them. Designing a compact and scalable methodology that utilises the special structure of costs to determine the costs of all experts in a computationally efficient manner is an open problem.

## 7 Conclusion

We consider the task of cost-sensitive binary classification using a local model that works in conjunction with a more accurate but costly remote model. We use the HI framework, where each sample is first sent to the local model, and the decision to offload to the remote model is made based on the output of the local model. For calibrated local classifiers, we derived a Bayes optimal two-threshold rule. For general, uncalibrated models, we developed H2T2, an online learning policy that finds the optimal thresholds with partial feedback and has sublinear regret. Unlike previous HI learning algorithms that use a single threshold for uniform misclassification costs, H2T2 uses two thresholds to handle asymmetric costs and creates an ambiguity region for the offloading decision. It also makes its own cost-sensitive local inferences. H2T2 is a novel approach because it operates during the inference phase without requiring LDL retraining to improve the classification accuracy. It is also agnostic to the models being used. Simulations across various datasets and models show that H2T2 consistently outperforms naive, single-threshold, and even offline single-threshold policies. While certain dataset-model combinations might favor naive policies, these conditions are unknown beforehand and are vulnerable to OOD data. H2T2 is a robust and flexible solution for OOD data, making it ideal for real-world applications.

## References


Al-Atat, G.; Datta, P.; Moharir, S.; and Champati, J. P. 2024. Regret bounds for online learning for hierarchical inference. In *Proceedings of the 25th MobiHoc '24*, 281–290. ACM.

Al-Atat, G.; Fresa, A.; Behera, A. P.; Moothedath, V. N.; Gross, J.; and Champati, J. P. 2023. The Case for Hierarchical Deep Learning Inference at the Network Edge. In *Proceedings of the 1st NetAISys*. ACM.

Behera, A. P.; Daubaris, P.; Bravo, I.; Gallego, J.; Morabito, R.; Widmer, J.; and Champati, J. P. 2025. Exploring the Boundaries of On-Device Inference: When Tiny Falls Short, Go Hierarchical. *IEEE Internet of Things Journal*, 1–1.

Beytur, H. B.; Aydin, A. G.; de Veciana, G.; and Vikalo, H. 2024. Optimization of Offloading Policies for Accuracy-Delay Tradeoffs in Hierarchical Inference. In *IEEE INFOCOM 2024*, 1989–1998.

Cesa-Bianchi, N.; and Lugosi, G. 2006. *Prediction, learning, and games*. Cambridge University Press. ISBN 978-0-511-54692-1.

Chow, C. 2003. On optimum recognition error and reject tradeoff. *IEEE Transactions on information theory*, 16(1): 41–46.

Cortes, C.; DeSalvo, G.; and Mohri, M. 2016. Learning with rejection. In *27th International conference, ALT*, 67–82. Springer.

Datta, P.; Moharir, S.; and Champati, J. P. 2025. Online Learning with Stochastically Partitioning Experts. In *Proc. UAI*.

Elkan, C. 2001. The foundations of cost-sensitive learning. In *IJCAI*, 973–978. Lawrence Erlbaum Associates Ltd.

Kermany, D. 2018. Labeled optical coherence tomography (oct) and chest x-ray images for classification. *Mendeley data*.

Krizhevsky, A. 2009. The CIFAR-10 dataset.

Krizhevsky, A.; Hinton, G.; et al. 2009. Learning multiple layers of features from tiny images.

Letsiou, A.; Moothedath, V. N.; Behera, A. P.; Champati, J. P.; and Gross, J. 2024. Hierarchical Inference at the Edge: A Batch Processing Approach. In *2024 IEEE/ACM SEC*, 476–482.

Mohamed, H. 2025. Chest CT-Scan images Dataset.

Moothedath, V. N.; Champati, J. P.; and Gross, J. 2024. Getting the Best Out of Both Worlds: Algorithms for Hierarchical Inference at the Edge. *IEEE Transactions on Machine Learning in Communications and Networking*, 2: 280–297.

Narasimhan, H.; Jitkrittum, W.; Menon, A. K.; Rawat, A.; and Kumar, S. 2022. Post-hoc estimators for learning to defer to an expert. *Advances in Neural Information Processing Systems*, 35: 29292–29304.

Ni, C.; Charoenphakdee, N.; Honda, J.; and Sugiyama, M. 2019. On the calibration of multiclass classification with rejection. *Advances in neural information processing systems*, 32.

Nikoloska, I.; and Zlatanov, N. 2021. Data Selection Scheme for Energy Efficient Supervised Learning at IoT Nodes. *IEEE Comm. Let.*, 25(3): 859–863.

Ramaswamy, H. G.; Tewari, A.; and Agarwal, S. 2018. Consistent algorithms for multiclass classification with an abstain option. *Electronic Journal of Statistics*, 12(1): 530 – 554.

Saerens, M.; Latinne, P.; and Decaestecker, C. 2002. Adjusting the outputs of a classifier to new a priori probabilities: a simple procedure. *Neural computation*, 14(1): 21–41.

Spanhol, F. A.; Oliveira, L. S.; Petitjean, C.; and Heutte, L. 2015. A dataset for breast cancer histopathological image classification. *Ieee transactions on biomedical engineering*, 63(7): 1455–1462.

Sturzinger, E.; and Satyanarayanan, M. 2024. Beyond Federated Learning: Survival-Critical Machine Learning. In *2024 IEEE/ACM SEC*, 483–489. IEEE.

Tan, C. L. 2018. Phishing dataset for machine learning: Feature evaluation. *Mendeley Data*, 1(8).

Tiwari, S. 2025. Phishing Dataset for Machine Learning.

# A Proofs

**Proof of Theorem 1 on page 3:** Define optimal predictor as the one minimizing the expected LDL cost. Let $Y$ denote random variable $h_r(X)$. Recall $\phi_t$ from (1) and $f_t \coloneqq f_1(x_t)$.

$$\begin{aligned}\mathbb{E}[\phi_t] &= \mathbb{E}_X\big[\delta_1 \mathbb{1}_{h_l(X)=1}\mathbb{P}(Y=0 \mid X) \\ &\quad + \delta_{-1}\mathbb{1}_{h_l(X)=0}\mathbb{P}(Y=1 \mid X)\big], \\ &= \mathbb{E}_X\big[\delta_1 \mathbb{1}_{h_l(X)=1}(1-f(X)) + \delta_{-1}\mathbb{1}_{h_l(X)=0}f(X)\big],\end{aligned}$$

where $\mathbb{1}_{\cdot}$ is the indicator function. It follows that the optimal predictor of the calibrated LDL denoted by $h_l^*(X)$ activates the indicator function that minimizes $\mathbb{E}[\phi_t]$. That is,

$$h_l^*(X) = \begin{cases} 1, & \text{if} \quad \Rightarrow f(X) \geq \frac{\delta_1}{\delta_1+\delta_{-1}}, \\ 0, & \text{otherwise}, \end{cases}$$

as given in (6). Thus, with this optimum predictor, we get:

$$\mathbb{E}[\phi_t] = \min\{\delta_1(1-f_t), \delta_{-1}f_t\}.$$

Now, let $\mathbb{I}_t$ denote the indicator random variable denoting the decision to offload sample $x_t$. Then we have the cost $l_t$:

$$l_t = \beta_t \mathbb{I}_t + \phi_t(1-\mathbb{I}_t)$$

with an the optimum decision is to offload if $\beta_t < \mathbb{E}[\phi_t]$. That is, for calibrated LDL with optimal predictor, the optimum decision is to offload when

$$\begin{aligned}&\beta_t < \min\{\delta_1(1-f_t), \delta_{-1}f_t\}, \\ \Rightarrow\ &\theta_l^{*(t)} = \tfrac{\beta_t}{\delta_{-1}} < f_t < 1 - \tfrac{\beta_t}{\delta_1} = \theta_u^{*(t)},\end{aligned}$$

with an associated expected cost given by (8). □

**Proof of Lemma 1 on page 4:** Taking expectation of $\hat{l}$ over realizations of $\zeta$ gives

$$\begin{aligned}\mathbb{E}_\zeta[\tilde{l}_t(\vec{\theta})] &= \mathbb{1}_{f_t \notin [\theta_l,\theta_u]} \cdot \mathbb{P}(\zeta=1)\tfrac{\phi_t}{\epsilon} + \mathbb{1}_{\theta_l<f_t<\theta_u} \cdot \beta_t, \\ &= \mathbb{1}_{f_t \notin [\theta_l,\theta_u]} \cdot \phi_t + \mathbb{1}_{\theta_l<f_t<\theta_u} \cdot \beta_t = l_t(\vec{\theta}).\end{aligned}$$ □

**Proof of Lemma 2 on page 5:** We have,

$$\mathbb{E}\left[L_T\right] = \sum_{t=1}^{T}\sum_{\vec{\theta}\in\Theta} \tfrac{w_t(\vec{\theta})}{W_t}\mathbb{E}_{\zeta_t}\left[l_t(\vec{\theta})\right], \tag{14}$$

$$\mathbb{E}\left[\tilde{L}_T\right] = \sum_{t=1}^{T}\sum_{\vec{\theta}\in\Theta} \tfrac{w_t(\vec{\theta})}{W_t}\mathbb{E}_{\zeta_t}\left[\tilde{l}_t(\vec{\theta})\right]. \tag{15}$$

If a policy chooses $\vec{\theta} = (\theta_l, \theta_u)$ in round $t$, the loss is

$$l_t(\vec{\theta}) = \mathbb{1}_{f_t \notin [\theta_l,\theta_u]}\mathbb{1}_{\zeta_t=0}\phi_t + \left(1 - \mathbb{1}_{f_t \notin [\theta_l,\theta_u]}\mathbb{1}_{\zeta_t=0}\right)\beta_t.$$

Using $l_t(\vec{\theta}) = \mathbb{1}_{f_t \notin [\theta_l,\theta_u]}\phi_t + \left(1 - \mathbb{1}_{f_t \notin [\theta_l,\theta_u]}\right)\beta_t$ from (3) and taking expectation on both sides, we get,

$$\begin{aligned}&\mathbb{E}_\zeta\left[l_t(\vec{\theta})\right] - l_t(\vec{\theta}) = \epsilon\mathbb{1}_{f_t \notin [\theta_l,\theta_u]}(\beta_t - \phi_t). \\ \Rightarrow\ &\mathbb{E}_\zeta\left[l_t(\vec{\theta})\right] - \mathbb{E}_\zeta\left[\tilde{l}_t(\vec{\theta})\right] = \epsilon\mathbb{1}_{f_t \notin [\theta_l,\theta_u]}(\beta_t - \phi_t) \leq \epsilon.\end{aligned}$$

In the last step, we used Lemma.1. Since this holds for any $\vec{\theta}$ and $t$, we have for any policy and time horizon $T$

$$\mathbb{E}\left[L_T\right] - \mathbb{E}\left[\tilde{L}_T\right] \leq \epsilon\beta_t T \leq \epsilon\beta T \leq \epsilon T.$$ □

**Proof of Theorem 2 on page 5:** Recall $\tilde{L}_T(\vec{\theta})$: the cumulative estimated loss with a fixed $\vec{\theta}$. Consider $\ln\frac{W_{T+1}}{W_1}$:

$$\begin{aligned}\ln\tfrac{W_{T+1}}{W_1} &= \ln\sum_{\vec{\theta}\in\Theta} e^{-\eta\sum_{t=1}^{T}\tilde{l}_t(\vec{\theta})} - \ln(|\Theta|), \\ &\geq -\min_{\vec{\theta}\in\Theta}\eta\tilde{L}_T(\vec{\theta}) - \ln(|\Theta|).\end{aligned} \tag{16}$$

Using Lemma 1 and Jensen's inequality on expectations:

$$\begin{aligned}\mathbb{E}_\zeta\left[\ln\tfrac{W_{T+1}}{W_1}\right] &\geq -\min_{\vec{\theta}\in\Theta}\eta\mathbb{E}_\zeta\left[\tilde{L}_T(\vec{\theta})\right] - \ln(|\Theta|) \\ &= -\min_{\vec{\theta}\in\Theta}\eta L_T(\vec{\theta}) - \ln(|\Theta|).\end{aligned} \tag{17}$$

Next, we upper bound $\log\frac{W_{T+1}}{W_1}$ as follows:

$$\begin{aligned}\ln\tfrac{W_{t+1}}{W_t} &= \ln\sum_{\vec{\theta}\in\Theta}\tfrac{w_t(\vec{\theta})}{W_t}e^{-\eta\tilde{\ell}_t(\vec{\theta})} \\ &\leq \ln\sum_{\vec{\theta}\in\Theta}\tfrac{w_t(\vec{\theta})}{W_t}\left(1 - \eta\tilde{\ell}_t(\vec{\theta}) + \left(\eta\tilde{\ell}_t(\vec{\theta})\right)^2/2\right) \\ &= \ln\left(1 + \sum_{\vec{\theta}\in\Theta}\tfrac{w_t(\vec{\theta})}{W_t}\left(-\eta\tilde{\ell}_t(\vec{\theta}) + \left(\eta\tilde{\ell}_t(\vec{\theta})\right)^2/2\right)\right).\end{aligned} \tag{18}$$

Simplifying, we get,

$$\ln \frac{W_{t+1}}{W_t} \leq \sum_{\vec{\theta}\in\Theta} \frac{w_t(\vec{\theta})}{W_t} \left(-\eta\tilde{\ell}_t(\vec{\theta}) + \left(\eta\tilde{\ell}_t(\vec{\theta})\right)^2/2\right) \tag{19}$$

$$\leq \sum_{\vec{\theta}\in\Theta} \frac{w_t(\vec{\theta})}{W_t} \left(-\eta\tilde{\ell}_t(\vec{\theta}) + \eta^2\tilde{\ell}_t(\vec{\theta})/2\epsilon\right). \tag{20}$$

Above, we have used $e^{-x} \leq 1 - x + \frac{x^2}{2}$, $\ln(1+x) \leq x$, and $\tilde{\ell}_t(\vec{\theta}) \leq \frac{1}{\epsilon}$ in (18), (19), and (20), respectively. Now we sum (20) telescopically over the entire horizon $T$ as follows:

$$\ln \frac{W_{T+1}}{W_1} = \ln \prod_{t=1}^{T} \frac{W_{t+1}}{W_t} = \sum_{t=1}^{T} \ln \frac{W_{t+1}}{W_t}, \tag{21}$$

$$\leq \sum_{t=1}^{T} \sum_{\vec{\theta}\in\Theta} \frac{w_t(\vec{\theta})}{W_t} \left(-\eta\tilde{\ell}_t(\vec{\theta}) + \frac{\eta^2\tilde{\ell}_t(\vec{\theta})}{2\epsilon}\right). \tag{22}$$

$$\Rightarrow \mathbb{E}\Big[\ln \frac{W_{T+1}}{W_1}\Big] \leq -\eta \sum_{t=1}^{T} \sum_{\vec{\theta}\in\Theta} \frac{w_t(\vec{\theta})}{W_t} \mathbb{E}_\zeta[\tilde{l}_t(\vec{\theta})] + \eta^2 \sum_{t=1}^{T} \sum_{\vec{\theta}\in\Theta} \frac{w_t(\vec{\theta})}{W_t} \frac{\mathbb{E}_\zeta[\tilde{l}_t(\vec{\theta})]}{2\epsilon}$$

$$\leq -\eta\mathbb{E}[\tilde{L}_T(\vec{\theta})] + \frac{\eta^2}{2\epsilon}T \tag{23}$$

$$\leq -\eta\mathbb{E}[L_T(\vec{\theta})] + \eta\epsilon\beta T + \frac{\eta^2}{2\epsilon}T. \tag{24}$$

In (23), we use $\mathbb{E}_\zeta[\tilde{l}_t(\vec{\theta})] = l_t(\vec{\theta}) \leq 1$ and the expectation is taken over expert selection and $\zeta$. In (24), we use Lemma 1. The result follows by comparing bounds from (17) and (24):

$$\eta\mathbb{E}[L_T(\vec{\theta})] - \min_{\vec{\theta}\in\Theta} \eta L_T(\vec{\theta}) \leq \eta\epsilon\beta T + \frac{\eta^2 T}{2\epsilon} + \log(|\Theta|).$$

Recall (5). Taking expectation over arrivals and $\phi_t$, we get:

$$R_T \leq \left(\epsilon\beta + \frac{\eta}{2\epsilon}\right) T + \frac{\log(|\Theta|)}{\eta}.$$

Corollary 1 follows by setting partial derivatives to zero. While not optimal, choosing $\eta = \left(2\ln^2(|\Theta|)/T^2\right)^{1/3}$ and $\epsilon = \sqrt{\eta/2}$ yields regret in the same order: $O(T^{2/3})$. □

**Proof of Theorem 3 on page 6:** Let random variables $X, Y$ and $\mathbb{1}_{\cdot}$ denote $x_t, h_r(x_t)$ and the indicator function.

$$\mathbb{E}[\phi_t] = \mathbb{E}_X \sum_{j=1}^{K} \mathbb{1}_{h_l(X)=j} \sum_{i=1}^{K} \mathbb{P}(Y = i \mid X) C_{ij},$$

$$= \mathbb{E}_X \sum_{j=1}^{K} \mathbb{1}_{h_l(X)=j} f^T C_j.$$

It follows that $h_l^*(X)$ activates the $j$ that minimizes $f^T C_j$:

$$h_l^*(X) = \arg\min_j f^T C_j,$$

with $\mathbb{E}[\phi_t] = \min_j f^T C_j$. Now, let $\mathbb{I}_t$ denote the decision to offload $x_t$. We have, $l_t = \beta_t\mathbb{I}_t + \phi_t(1 - \mathbb{I}_t)$. Thus, it is optimal to offload if $\beta_t < \mathbb{E}[\phi_t]$. That is, for calibrated LDL with optimal predictor, it is optimal offload when $\beta_t < \min_k\{f^T C_k\}$, with $\mathbb{E}[l_t] = \min\{\beta_t, \min_k f^T C_k\}$. □

| Dataset | Test Size | LDL | Accuracy | FP | FN |
|---|---|---|---|---|---|
| BreakHis | 3365 | MobileNet-based | 72% | 10% | 18% |
| Chest | 278 | MobileNet-based | 64% | 16% | 20% |
| Phishing | 1106 | Logistic regression | 75% | 12% | 13% |
| Synthetic | $10^5$ | Naive | 66% | 15% | 19% |
| BreaCh† | 7909 | CNN | 45%† | 17% | 38% |
| ChestXRay | 624 | MobileNet-based | 78% | 18% | 4% |
| ResnetDogs | 2000 | ResNet | 73% | 15% | 11% |
| LogisticDogs | 2000 | Logistic regression | 56% | 22% | 22% |
| X-RaCT† | 5856 | Chest classifier | 35%† | 1% | 64% |

Table 3: Different dataset-model pairs used in this technical appendix. †Note that BreaCh and X-RaCT are OOD datasets.

# B Supplementary Matrial

In this appendix, we provide supplementary material containing results from additional dataset and results as shown below:

1. Extended dataset description
   (a) Datasets included in the manuscript
   (b) Additional datasets not included in the manuscript
      i. ResnetDogs: Dogs vs. Cats; Resnet-based LDL
      ii. LogisticDogs: Dogs vs. Cats; logistic regression-based LDL
      iii. ChestXRay: Pneumonia detection; CNN-based LDL
      iv. X-RaCT: Chest X-Ray data on CT Scan model (OOD configuration)
2. Additional numerical results
   (a) Average cost vs. $\beta \in (0,1)$, $\delta_1 = 0.7$, $\delta_{-1} = 1$
   (b) Average cost vs. $\beta \in (0,1)$, $\delta_1 = 0.25$, $\delta_{-1} = 1$
   (c) Average cost vs. cost asymmetry $\frac{\delta_1}{\delta_{-1}} \in (\frac{1}{10}, 10)$
   (d) Average cost vs. Learning rate $\eta$
   (e) Cost and time-complexity vs. LDL output quantization

## Dataset Description

Here, we present a detailed description of the datasets and classification models that we employed in the manuscript, as well as the additional ones that we used in this appendix. The same is also provided in TABLE 3.

**Breast Cancer Detection (Breakhis) Dataset** The Breast Cancer Histopathological Image Classification (BreakHis) dataset (Spanhol et al. 2015) consists of 7909 microscopic images of breast tumor tissue collected from 82 patients. The dataset contains 2480 benign (class 0) and 5429 malignant (class 1) cell images. 3365 random samples with 1877 malignant cell images are used for the final testing of the model; the rest are used for training purposes. The local model uses a MobileNet base model followed by a Flatten layer, Batch Normalization, a Dense(256, relu), Dropout(0.5), and finally a Dense layer with softmax for binary classification.

**Chest CT Scan Dataset** The Chest CT Scan dataset (Mohamed 2025) originally comprises images categorized into four classes: healthy or one of three distinct cancerous conditions. For the purpose of this study, the dataset was reformulated into a binary classification task that differentiates between cancerous (class 1) and healthy (class 0) cells, making it an unbalanced dataset towards class 1 with a ratio of 4:1. A total of 566 CT scan images were allocated for training the binary classification model, while an independent set of 278 CT scan images was used for testing. Prior to model training, standard pre-processing steps were applied to the CT images. The LDL model employed for inference is based on the MobileNet architecture. The complete model has a memory footprint of 13.34 MB, including 1.01 MB of trainable parameters.

**Phishing Dataset** The phishing dataset (Tiwari 2025; Tan 2018) utilized in our experiments comprises 48 ternary features corresponding to binary labels indicating the presence or absence of phishing activity. The dataset includes data extracted from 5000 confirmed phishing websites and 5000 legitimate websites. These webpages were collected during two periods: January to May 2015 and May to June 2017. To maintain a lightweight LDL model suitable for deployment on resource-constrained end devices, we restrict the input feature set to 13 of the 48 available features, where each selected feature is ternary-valued, taking on one of three possible states: $+1$, $0$, or $-1$. The classification output is binary, with labels $+1$ or $-1$ (which we convert to 1 and 0), indicating phishing or legitimate webpages, respectively. The dataset consists of 11,054 labeled entries. For model development, an 80-20 train-test split is applied. A logistic regression model that occupies 56 bytes of memory is trained using this data to simulate the LDL inference mechanism. A separate set of 1106 samples is reserved for evaluating the performance of the offloading policies under study.

**Synthetic Dataset** We used a synthetic dataset to illustrate the FPR-FNR regions, where the regions are smooth and easy to understand in Fig.2 in the Introduction of the manuscript, to assist the reader. We created this dataset by generating the softmax values using a gaussian mixture model by generating sampling according to distributions $\mathcal{N}(0.9, 0.4)$ and $\mathcal{N}(0.3, 2)$ corresponding to class 1 and 0 respectively, followed by cherry-picking equal number of valid values in $(0, 1)$.

Note that the synthetic dataset is ignored in this technical appendix from here on, and we will only show real datasets.

**ChestXRay** The Chest X-ray Pneumonia (Kermany 2018) dataset consists of 5,216 training X-ray images with 1,341 normal and 3,875 pneumonia (class 1), and 624 test images (234 normal and 390 pneumonia), with an additional 16 images for validation. A lightweight convolutional neural network with three convolutional layers, max pooling, and global average pooling was trained for binary classification.

**ResnetDogs** We used a subset of the CIFAR-10 (Krizhevsky, Hinton et al. 2009; Krizhevsky 2009) dataset containing only cat and dog images, with 10,000 training images (80% train, 20% validation) and 2,000 test images equally split between the two classes. A compact ResNet-8 model with four residual blocks, batch normalization, and global average pooling was trained for binary classification.

**LogisticDogs** We used the same CIFAR-10 dataset as above, but used a logistic regression model as the LDL. This model occupies 97 KB of memory and was trained on flattened and standardized image pixels using a Scikit-learn pipeline.

**BreaCh** BreaKhis-dataset-on-ChestCTScan-model, or BreaCh, is created by classifying all 7909 BreakHis samples using the model trained on Chest CT scan (Mohamed 2025). It mimics an OOD data scenario with a domain shift for the model trained on the Chest CT scan. As a result, unbeknownst to the user, the accuracy drops below 50%, resulting in the misdiagnosis of 38% cancerous tumors.

**X-RaCT** X-Ray-dataset-on-ChestCTScan-model, or X-RaCT, is created by classifying all 5856 X-Ray images from Kermany (2018) using a chest CT Scan model created originally for training on the Mohamed (2025) dataset. As with the BreaCh dataset above, this mimics OOD data, and the accuracy drops much below a random predictor. One can, of course, invert it to get better-than-random results, but we assume that the mistake is unknown to the user. Nonetheless, rather than its plausibility, we use it to illustrate the data, model, or distribution mismatch.

## Additional Numerical Results.

We will show additional numerical results in the coming pages. We will provide a detailed description in the figure caption for the convenience of the reader.

1. In Fig. 6, we show average cost vs. $\beta$ for additional datasets that were not shown in the manuscript. We use $\delta_1 = 0.7, \delta_{-1} = 1, T = 10000$. Additionally, we show the full range of $\beta \in (0, 1)$ here, while in the manuscript this was restricted to $\beta \in (0, 0.6)$ to highlight the lower transitional region of the offloading cost.
2. In Fig. 7, we show average cost vs. $\beta$ for all datasets for a different misclassification cost settings. We use $\delta_1 = 0.25, \delta_{-1} = 1, T = 10000$.
3. In Fig. 8, we show the average cost vs. the amount of asymmetry between FN and FP in terms of the ratio $\frac{\delta_1}{\delta_{-1}}$, which is used to show this asymmetry. Here we illustrate that the performance gains of the two-threshold policies–and by extension H2T2–increase with an increase in asymmetry.
4. In Fig. 9, we show the effect of learning rate $\eta$ on the average cost. As we have described in the manuscript, the bound optimising learning rate might not be the one that provides minimum regret, and we chose $\eta = 1$ for simplicity. We use this figure to illustrate this.
5. ***Resolution vs. run time***: In Fig. 10, we show the average cost and runtime of the algorithms with different

quantizations $b$ that result in different LDL output resolution. We use this figure to argue that $b = 4$ used in the manuscript is a good trade-off.

**Computational Complexity:** H2T2 comes with two internal steps: the decision making step with $O(|\Theta|)$ number of summations; and the weight updation step with a $O(|\Theta|)$ number of multiplications.

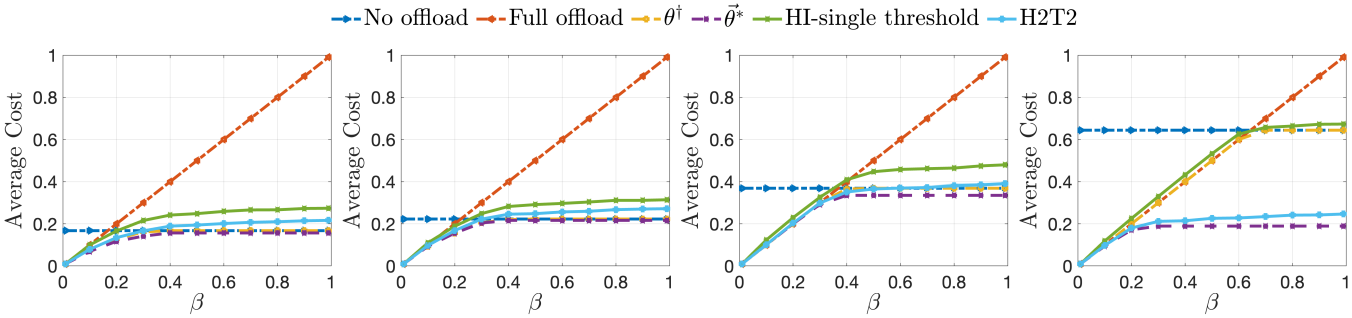


Figure 6: **Average cost vs. $\beta$ for datasets not shown in the original manuscript**. We use $\delta_1 = 0.7, \delta_{-1} = 1, T = 10000$. Subfigure numbering is kept (d)-(h) for consistency with other figures.

We show the full range of $\beta \in (0, 1)$ here, while in the manuscript this was restricted to $\beta \in (0, 0.6)$ to highlight the lower transitional region of the offloading cost. As $\beta$ increases, it becomes more and more obvious that a no-offload policy would do better. On the other hand, an online learning policy would have to incur the exploration cost of $\epsilon\beta$, even after convergence to the optimum $\vec{\theta}$. That being said, H2T2 attains a cost very close to the minimum when the cost settings favour any naive policies like full-offload or no-offload, thereby not incurring a substantial regret for not choosing them. Further, while the online learning policies automatically converge close to those costs, the regions where these naive policies become better are not known a priori, and a user is unable to choose this beforehand.

Also note that for general settings, both single threshold offline optimum and two-threshold offline optima ($\theta^\dagger$ and $\vec{\theta}^*$) attain the same cost as the no-offload policy for large $\beta$ close to 1. However, for the OOD (Out Of Distribution) data – BreaCh and X-RaCT – two-threshold policies can provide a much smaller cost than single-threshold policies. Even in such OOD datasets, H2T2 follows the optimum offline two-threshold policy very closely.

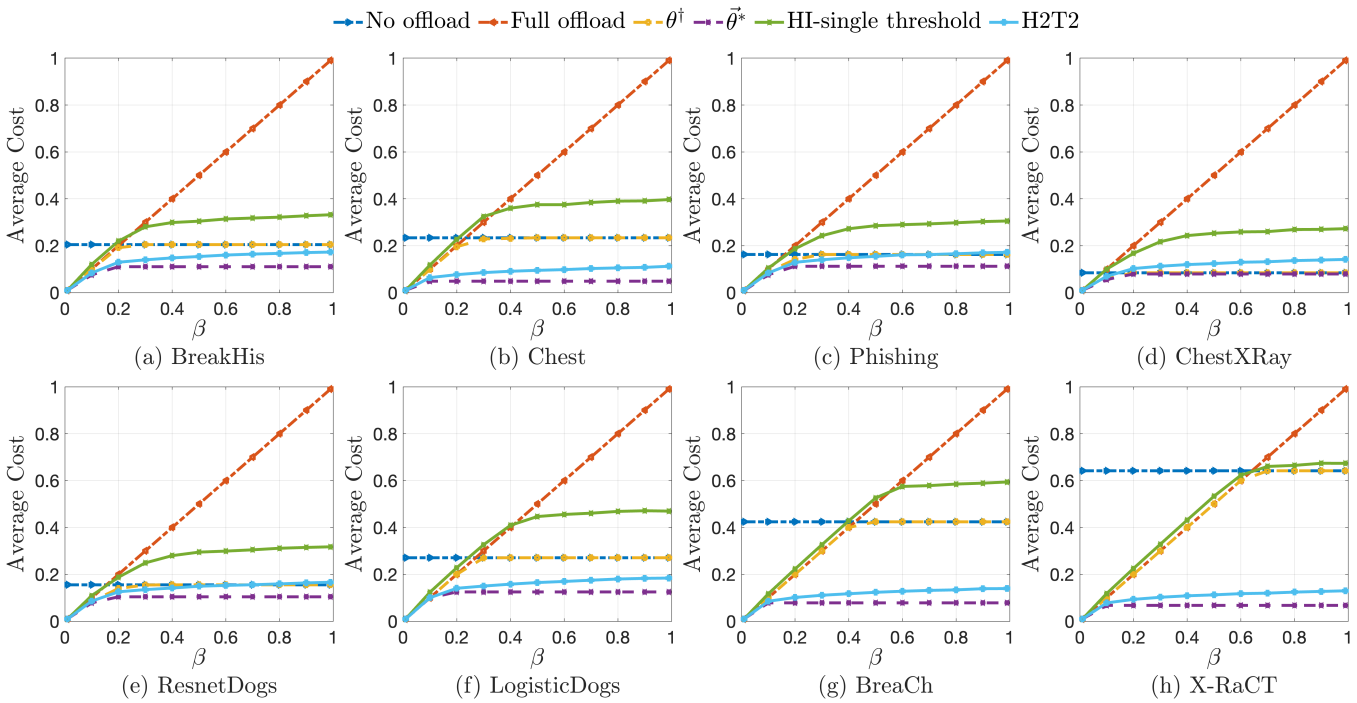


Figure 7: **Average cost vs. $\beta$ for different misclassification costs from what is provided in the manuscript**. We use $\delta_1 = 0.25, \delta_{-1} = 1, T = 10000$.

Note, in particular the ResnetDogs and LogisticDogs in (e) and (f), respectively. Here we classify the same data using two different models with roughly 17% difference in accuracies. This is also reflected in the costs of their respective No-offload policies. However, in both cases, H2T2 performs relatively similar in terms of costs.

Further, Compare with Fig.6 from this technical appendix. The performance gain of H2T2 increases when the misclassification costs get increasingly asymmetric. This further justifies the applicability of H2T2 in the setting that we considered, such as medical and surveillance.

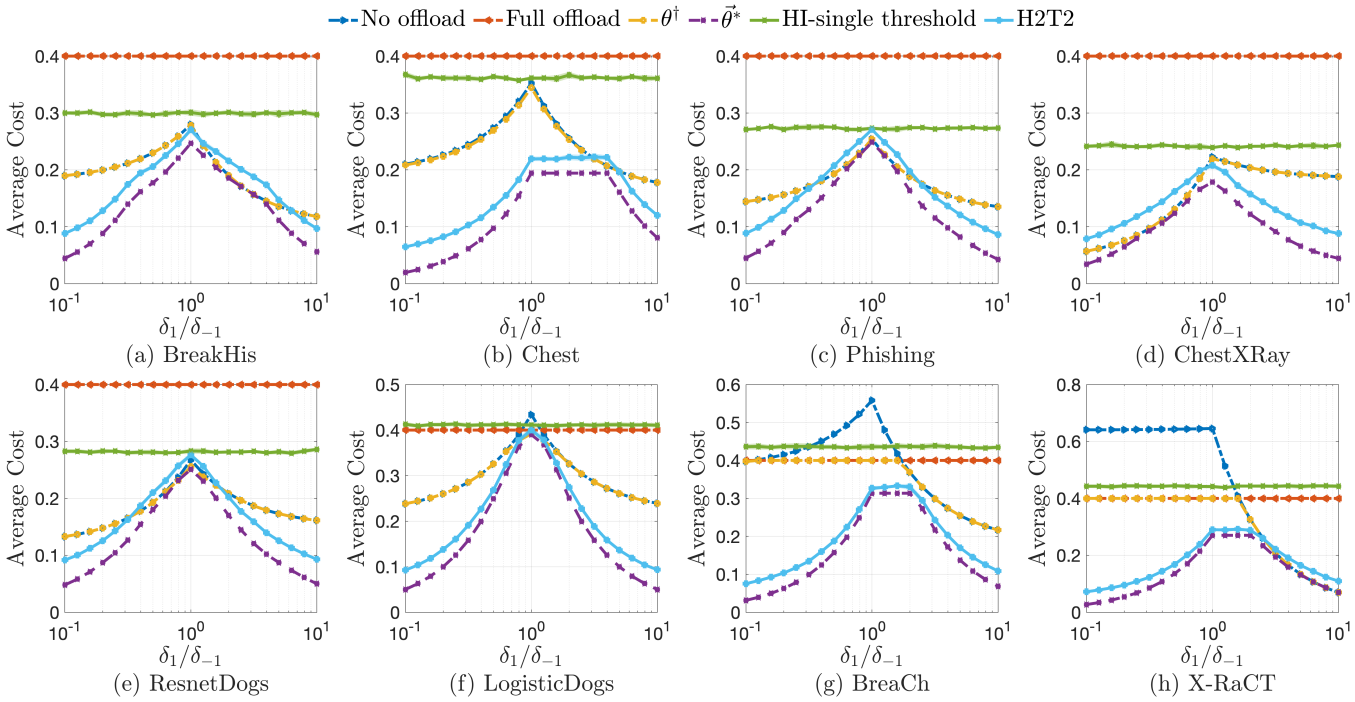


Figure 8: **Average cost vs. the amount of asymmetry between FN and FP.** Here, we show the average cost incurred for different policies for varying asymmetry in misclassification costs framed as a ratio $\frac{\delta_1}{\delta_{-1}}$. We use $\beta = 0.4, T = 10000$.

The concavity of the curves is a result of the symmetry (between left and right side) in local models in terms of false positive and false negative rate. In models with class imbalance–such as the Chest dataset–this symmetry is not present.

HI–a policy that ignores cost asymmetry–incurs a fixed cost, and so does the Full-offload policy. H2T2, being capable of handling asymmetry, improves the costs as the asymmetry increases, and closely follows the offline tw-threshold optimum that attains the least cost throughout.

Further $\frac{\delta_1}{\delta_{-1}} = 1$ corresponds to no cost asymmetry. At this setting, as expected, H2T2 goes very close to, or equal to, HI-single threshold policies. However, the gap is noticeable for OOD data.

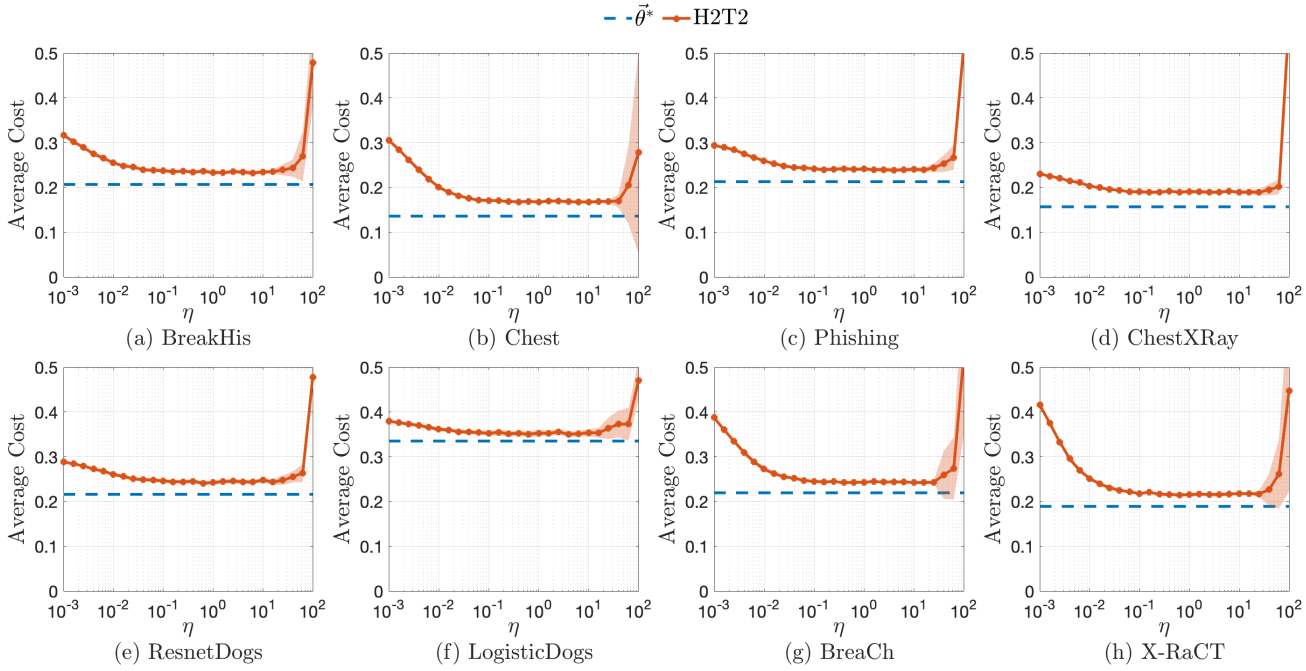


Figure 9: **Average cost vs. learning rate** $\eta$. We use $\beta = 0.4, \delta_1 = 0.7, \delta_{-1} = 1, T = 10000$. Similar trends were observed throughout the range of $\beta \in (0, 1)$.
As we have described in the manuscript, $\eta^*$ from Corollary 1–which in this case is $\sim 0.011$– that minimizes the worst-case regret bound, is not necessarily the one that provides minimum regret in a given setting. We use this figure to illustrate this. Further, while we chose $\eta = 1$ in the manuscript for simplicity without any parameter search, we could see that this choice is rather a good one.

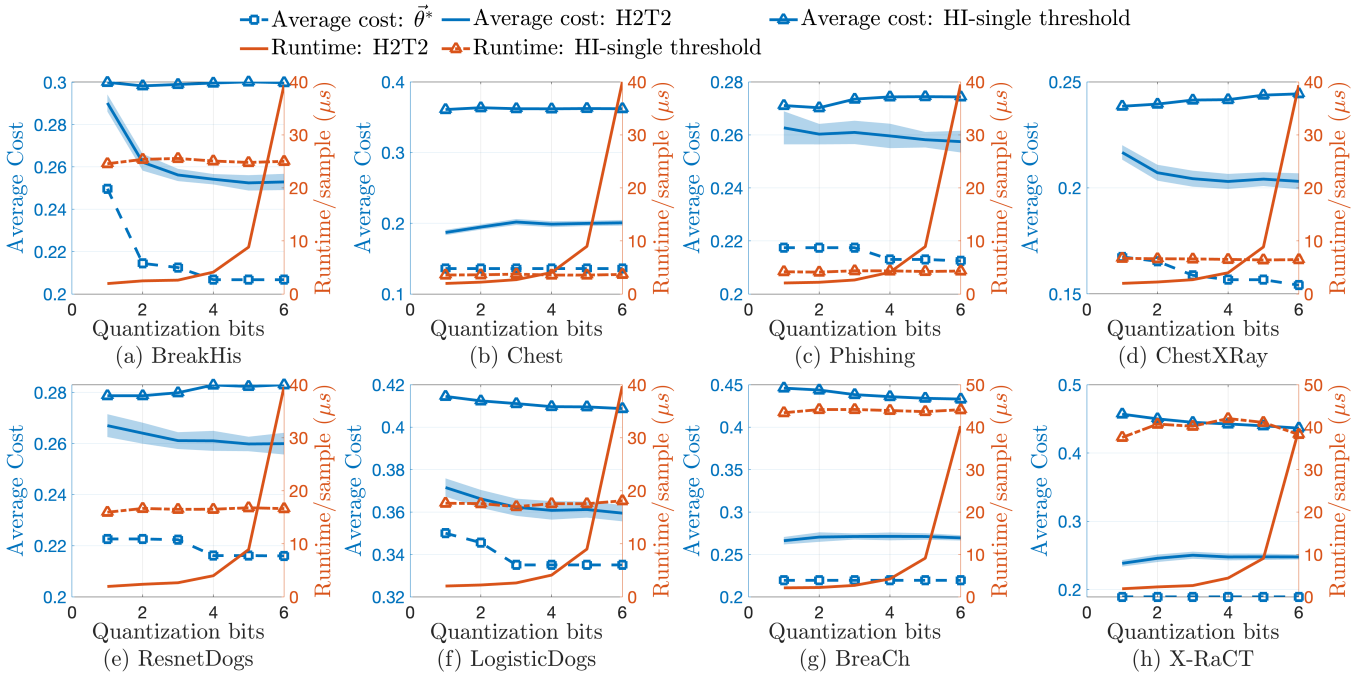


Figure 10: **Average cost and runtime-complexity with LDL output quantization**. We show the variation of average cost (left y-axis) and runtime (right y-axis) with the quantization in bits for different datasets. A $b$-bit quantization corresponds to a $2^{-b}$ resolution and number of experts $|\Theta| = 2^{b-1}(2^b + 1)$ after ignoring the invalid region.

As a result of the quantization, note that for smaller $b$, H2T2 performs faster than the single-threshold HI that employs a continuum expert without any quantization. However, as $b$ increases, H2T2 takes more time to run in comparison to the state-of-the-art single threshold HI; an expected behavior due to the increase in the dimensionality of the expert space. However, also note that H2T2 often does not require too small a resolution for the datasets studied, as observed from the flat average cost regions.

We see a good trade-off at $b = 4$, where the complexity is smaller than or comparable to the HI-single threshold, and the average cost has attained a fair amount of stability. This is the reason we used $b = 4$ in the manuscript.